Volume 18, Number 2, 2025. pp. 157-164

Jordan Journal of Physics

ARTICLE

Utilizing Semi-Empirical Miedema's Model for Gibbs Free Energy Calculations in Fe-Al-Cr and Fe-Al-Cu Alloys

Ali Kadhim Alsaedi[a], **Ahmed Rahem Karrawi**[b], **Hussien Abid Ali Bakir Mraity**[a] and **Faeq A. Al-Temimei**[a]

[a] *Department of Physics, Faculty of Science, University of Kufa, Najaf, Iraq.*
[b] *Faculty of dentistry, University of Kufa, Najaf, Iraq.*

Doi: **https://doi.org/10.47011/18.2.5**
Received on: 31/10/2023; *Accepted on: 14/03/2024*

Abstract: The Miedema semi-empirical model represents a promising technique for estimating the Gibbs free energy ***(ΔG)*** in Fe-Al-Cr and Fe-Al-Cu alloys. In this study, the software Materials Analysis Applying Thermodynamics (MAAT) was utilized to calculate ***ΔG***. The results indicated that the ***ΔG*** values for the binary alloys (Fe-Al, Fe-Cr, Al-Cr, and Al-Cu) were negative and lower than the ideal Gibbs free energy ***(ΔG^{ideal})***, except for Fe-Cu, which exhibited a positive ***ΔG***. For the ternary alloys (Fe-Al-Cr and Fe-Al-Cu), the ***ΔG*** values were predominantly negative across a wide range of compositions. This suggests the presence of driving forces promoting the formation of solid solutions from Fe, Al, Cr, and Cu throughout the entire composition range.

Keywords: Miedema's model, Gibbs free energy, FeAlCr, FeAlCu alloys.

1. Introduction

The thermodynamic properties of ternary alloys are crucial for understanding their phase behavior and relative stability. However, conducting experiments to determine these properties is challenging and time-consuming. Theoretical findings obtained through the application of Miedema's model can offer valuable information about the thermodynamic behavior of alloys [1]. Miedema's model is widely used to calculate the thermodynamic properties of binary and ternary alloys [2, 3]. It utilizes parameters such as electronegativity, electron density, and molar volume to calculate ***(ΔG)***.

Iron-aluminum (Fe-Al) alloys hold significant technological importance with promising properties. However, their limited ductility at ambient temperatures and reduced strength at high temperatures have hindered their widespread use in structural applications. Recent studies have focused on improving their mechanical properties through composition control, microstructure manipulation, and the addition of suitable alloying elements [4].

Fe-Al-Cr alloys are renowned for their exceptional resistance to oxidation at elevated temperatures, attributed to the formation of a protective alumina scale. These alloys are commonly used in heating foils, wires, and automotive catalyst supports [4]. Strengthening the dispersion and controlling grain size are effective approaches for enhancing their mechanical properties at high temperatures, and these methods are commonly applied in commercial production via powder metallurgy techniques [5]. Extensive research has been conducted on the structural and microstructural

Corresponding Author: Ali Kadhim Alsaedi **Email**: Alik.alsaaedi@uokufa.edu.iq

changes in mechanically alloyed Fe-Al-Cr powder mixtures.

Aghili *et al*. investigated the formation and structural changes in $Fe_{50}Cr_{25}Al_{25}$ powder particles and observed the generation of a composite lamellar structure of Fe, Cr, and Al with the dissolution of Al and Cr atoms in the Fe lattice [6]. In another study, Liu *et al*. reported the formation of a solid solution of Fe-Cr(Al) through Al diffusion into Fe-20Cr in nanocrystalline powders of Fe-40Al-5Cr [7].

Al-Cu-Fe alloys are notable for their low toxicity, availability, and cost-effectiveness [8]. The Al-Cu-Fe quasicrystalline phase has been widely used as a reinforcement to create composites with excellent mechanical and tribological properties [9-12]. Several publications have focused on the fabrication of Al-Cu-Fe quasicrystalline phases through mechanical alloying (MA) with or without subsequent annealing treatments. For example, direct formation of the quasicrystalline phase was achieved in $Al_{65}Cu_{20}Fe_{15}$ alloy after 15 hours of milling [12,13]. Mitka *et al*. studied the impact of mechanical alloying variables on phase formation in the $Al_{62}Cu_{25.5}Fe_{12.5}$ alloy and observed a mixture of icosahedral quasicrystal and β-Al(Cu, Fe) phases after 20 hours of milling at 300 rpm [13].

Travessa *et al*. found that the quasicrystalline phase could not be directly obtained in the $Al_{65}Cu_{20}Fe_{15}$ alloy [14]. Other studies have investigated the phase reactions during ball milling of $Al_{65}Cu_{23}Fe_{12}$, noting complex solid-state transformations upon annealing of the as-milled sample. These phase transformation results were linked to variations in the thermodynamic driving forces, including the positive heat of mixing for the Cu-Fe system and negative heats of mixing for the Al-Fe and Al-Cu systems [15]. This work aims to calculate the thermodynamic properties of Fe-Al-Cr and Fe-Al-Cu alloys employing the semi-empirical Miedema's model.

Gibbs Free Energy (ΔG)

Elucidating the practical implications of the highest and lowest Gibbs free energy ($\boldsymbol{\Delta G}$) values recorded in binary systems is essential for understanding how these values can impact alloy properties and applications. Also, the $\boldsymbol{\Delta G}$ values can be used to construct phase diagrams, which are essential for predicting the phases present in an alloy at different temperatures and compositions. This is valuable for alloy design and understanding how an alloy's composition affects its properties [16, 17].

The Gibbs free energy can be calculated using the equation:

$$\boldsymbol{\Delta G = \Delta H + T\Delta S} \quad (1)$$

where $\boldsymbol{\Delta H}$ is the mixing enthalpy change, $\boldsymbol{\Delta s}$ is the mixing entropy change, and $\boldsymbol{T}$ is the absolute temperature of the solid solution.

If we consider only entropy, the change in mixing entropy for the solid solution can be calculated using the following formula:

$$\boldsymbol{\Delta S = -R(X_A lnX_A + X_B lnX_B)} \quad (2)$$

$$\boldsymbol{X_A + X_B = 1}$$

where R is the universal gas constant and X_A and X_B are atomic concentrations in the solid solution.

2. Miedema's Model

The estimation of formation enthalpy ($\boldsymbol{\Delta H}$) is a valuable tool provided by the Miedema model. Initially developed for binary alloys, efforts have been made to extend it to ternary systems [18-20]. In this model, Wigner-Seitz cells form the basis of the binary alloy hypothesis. As pure metal atoms combine to form alloys, the boundaries of the Wigner-Seitz cells change. Miedema's model proposes two mechanisms contributing to the formation enthalpy of binary alloy systems. The first mechanism is directly proportional to $(\Delta\boldsymbol{\varphi}^*)^2$, which represents the charge transfer between neighboring cells resulting from attractive forces. The second mechanism is proportional to $(\Delta\boldsymbol{n_{ws}^{2/3}})$, which takes into account the repulsive forces arising from surface tension. The negative impact of $(\boldsymbol{\varphi}^*)$ and the positive effect of $(\Delta\boldsymbol{n_{ws}^{1/3}})$ determine their contributions to the mixing enthalpy [21, 22].

The equation representing $\boldsymbol{\Delta H}$ of a binary system can be formulated using the Miedema model [21-23]:

$$\boldsymbol{\Delta H_{AB}^{total} = \Delta H_{AB}^{chemical} + \Delta H_{AB}^{elastic} + \Delta H_{AB}^{structural}} \quad (3)$$

where $\boldsymbol{\Delta H^{chemical}}$ refers to the chemical contribution, $\boldsymbol{\Delta H^{elastic}}$ represents the elastic enthalpy, and $\boldsymbol{\Delta H^{Stractural}}$ refers to the structural

enthalpy resulting from the crystal structure difference of the binary system. In this regard, structural enthalpy is negligible due to its minimal effect on the total enthalpy [24].

The chemical enthalpy results from a difference in the binding energy of atoms in their initial elemental states compared to their mixed alloy states.

The following equation can determine the chemical enthalpy term for each binary system [23]:

$$\Delta H_{A\ in\ B}^{Chemical} = 2k\, X_A^S X_B^S\, C(x) \frac{(X_A\, V_A^{2/3} + X_B\, V_B^{2/3})}{(n_{ws}^A)^{-1/3} + (n_{ws}^B)^{-1/3}} \times \left[-(\Delta\emptyset^*)^2 + {}^{Q}/_{P}\left(\Delta n_{ws}^{1/3}\right)^2 - {}^{R^*}/_{P}\right] \quad (4)$$

where

$$\boldsymbol{X_A^S} = \frac{\boldsymbol{X_A\, V_A^{\frac{2}{3}}}}{\boldsymbol{X_A\, V_A^{\frac{2}{3}} + X_B\, V_B^{\frac{2}{3}}}} \quad (5)$$

$$\boldsymbol{X_B^S} = \frac{\boldsymbol{X_B\, V_B^{\frac{2}{3}}}}{\boldsymbol{X_A\, V_A^{\frac{2}{3}} + X_B\, V_B^{\frac{2}{3}}}} \quad (6)$$

To overcome the differences between the enthalpy of mixing obtained from Miedema's model and experimental data, Wang *et al.* [25] proposed a correction factor, ***C(x),*** which takes into account the atomic size of solvent and solute atoms.

$$\boldsymbol{C(x)} = \mathbf{1} - \boldsymbol{S}\frac{\boldsymbol{X_A X_A |V_A - V_B|}}{\boldsymbol{X_A^2 V_A + X_B^2 V_B}} \quad (7)$$

where S represents a semi-quantitative empirical variable that explains the influence of atomic size disparities. S equals 1 for a disordered solid solution. The liquid alloy and ordered compound S are considered equivalent to 0.5 and 2.0, respectively [26]. $\boldsymbol{V_{.A.}}$ and $\boldsymbol{V_{.B.}}$ are the molar volumes of ***A*** and ***B,*** respectively, $\boldsymbol{X_A}$ and $\boldsymbol{X_B}$ are the molar fractions of ***A*** and ***B***, respectively, $\boldsymbol{\Phi^*}$ is the constituent element work function, and $\boldsymbol{n_{ws}}$ is the density of electrons. ***P***, ***Q***, and ***R**** are known to be constants. ***P*** can be equal to 14.2 or 10.7, depending on whether the metals are transition or non-transition. Additionally, the value of ***P/Q*** was obtained to be 9.4. The ***R**** is an additional parameter for the enthalpy for both transition and non-transition metals.

The $\boldsymbol{\Delta H^{elastic}}$ represents the elastic enthalpy caused by the atom-sized mismatch. It can be written as [27]:

$$\boldsymbol{\Delta H_{AB}^{elastic} = K_B G_A (X_A \Delta H_{B\ in\ A} + X_B \Delta H_{A\ in\ B})} \quad (8)$$

where ***K*** and ***G*** refer to the bulk and shear modulus, respectively.

The structural enthalpy results from the crystal structure difference of the binary system. The $\boldsymbol{\Delta H^{Structural}}$ refers to the transition metals, which tend to crystallize preferentially in one out of three crystallographic phases, namely, bcc, fcc, and hcp, based principally on the number of valence electrons (***Z***). For binary solutions of transition–transition elements with shared bonds, this approach can be applied. Bakker et al. proposed the following expression for structural enthalpy [28]:

$$\boldsymbol{\Delta H_{A\ in\ B}^{struct} = (E_B^{struct} - E_A^{struct}) + (Z_A - Z_B)\frac{\partial E^{struct}(B)}{\partial Z}} \quad (9)$$

where both $\boldsymbol{Z_A}$ and $\boldsymbol{Z_B}$ represent the valence electrons of ***A*** and ***B*** atoms, respectively, while $\boldsymbol{E_B^{struct}}$ and $\boldsymbol{E_A^{struct}}$ refer to the lattice stability of each crystal structure (bcc, fcc, and hcp).

The thermodynamic parameters needed to compute the formation enthalpies are provided in Table 1.

TABLE 1. The required parameters to compute the Gibbs free energy change.

Metal	$\emptyset^*[V]$	$n_{ws}^{1/3}\,[d.u]^{1/3}$	$V_m^{2/3}\,[cm]^2$	Atomic radius [pm]
Fe	4.93	1.77	3.7	126
Al	4.20	1.39	4.6	143
Cr	4.65	1.73	3.7	125
Cu	4.45	1.47	3.7	128

3. Results and Discussion

3.1 Fe-Al-Cr Alloy

The highest $\boldsymbol{\Delta G}$ value typically corresponds to the most thermodynamically stable phase under specific conditions, whereas the lowest $\boldsymbol{\Delta G}$ value indicates the least stable phase. This information is critical for phase selection in alloy design. Phases with lower $\boldsymbol{\Delta G}$ values are generally less stable and may undergo phase

transformations at relatively lower temperatures. Such transformations can significantly influence the alloy's mechanical and thermal properties..

The outcomes of the thermodynamic computations for the binary alloys at 298K are shown in Fig.1. The graph illustrates the values of the Gibbs free energy change (ΔG) and the ideal Gibbs free energy change (ΔG^{ideal}) for different compositions. It is observed that for all concentrations, the (ΔG) values of Fe-Al, Fe-Cr, and Al-Cr alloys are negative and lower than the ΔG^{ideal} values. This indicates a strong interaction between the Fe, Al, and Cr atoms in these alloys.

Specifically, looking at Table 2, it can be noted that the ΔG of Fe-Cr is -3.13 kJ/mol, indicating a negative Gibbs free energy change for the formation of Fe-Cr alloy. This, combined with the small mismatch between the atomic radii and electronegativity of Fe and Cr, suggests that the formation of Fe-Cr alloy is relatively easy and feasible in the context of mechanical alloying (MA). These findings emphasize the favorable thermodynamic conditions for the formation of Fe-Cr alloy and provide insights into the potential for their synthesis and application in materials processing.

TABLE 2. Gibbs free energy in kJ/mol and atomic size mismatch for Fe-Al, Fe-Cr, and Al-Cr.

Binary alloy	ΔG [kJ/mol]	Atomic size mismatch %
FeAl	-15.48	13.4
FeCr	-3.13	0.8
AlCr	-14.8	12.5

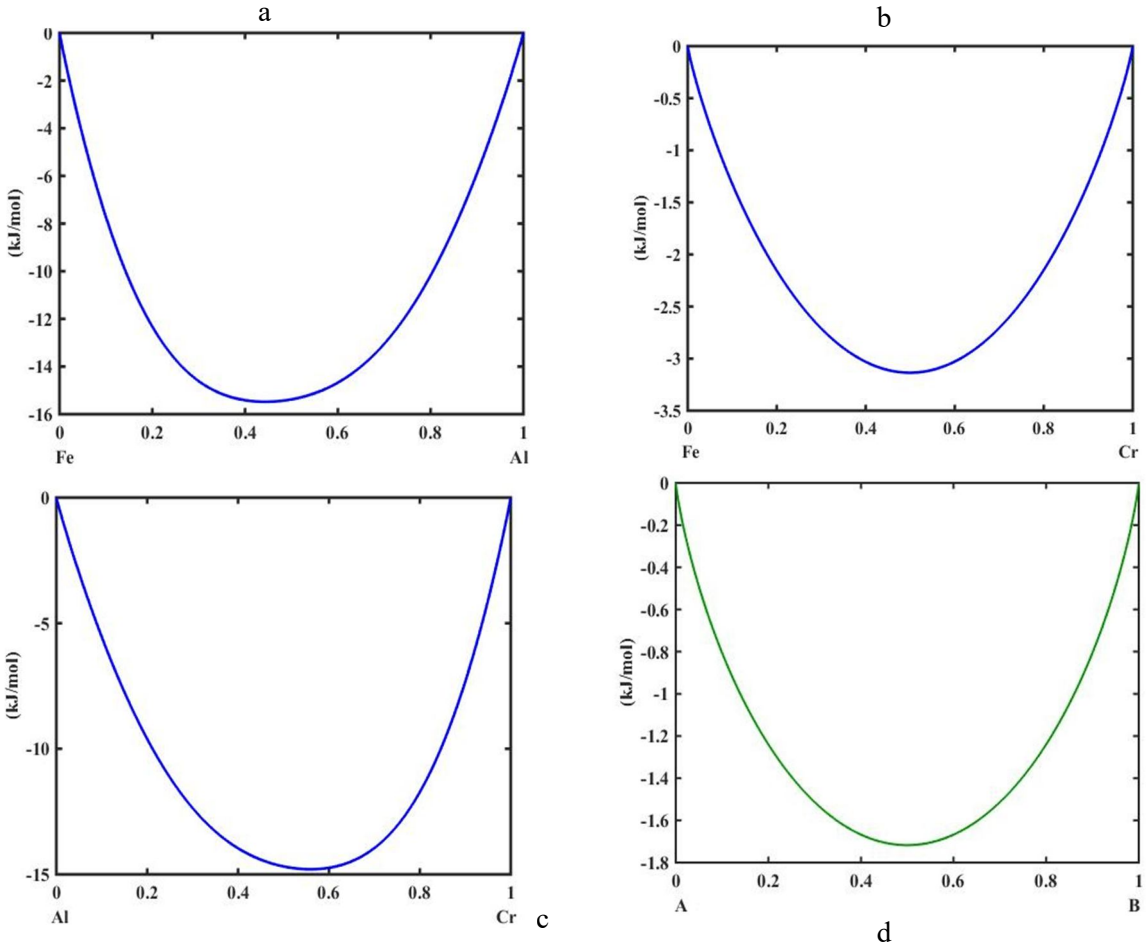

FIG. 1. Gibbs free energy of (a) Fe-Al, (b) Fe-Cr, and (c) Al-Cr alloys and (d) ideal Gibbs free energy.

The data presented in Fig. 2 provides valuable insights into the thermodynamic behavior of the Fe-Al-Cr alloy, specifically in terms of ΔG and ΔG^{ideal} values. The negative values of ΔG across the entire composition range indicate that there are driving forces promoting the formation of a solid solution from Fe, Al, and Cr. This implies that the thermodynamic conditions favor the mixing of these elements and the formation of a stable ternary alloy. The

negative ΔG values signify that the energy released during the formation of the solid solution exceeds the ideal energy required for a random mixture of the elements (ΔG^{ideal}). This suggests a favorable interaction between the Fe, Al, and Cr atoms within the ternary system.

It is worth noting that the largest ΔG values are observed in the vicinity of the Fe-Cr alloy. This indicates a relatively high energy release during the formation of Fe-Cr alloys, suggesting a stronger interaction between Fe and Cr atoms. Conversely, The Al-Cr alloy exhibits the lowest values of ΔG, indicating a lower energy release during the formation of Al-Cr alloy, suggesting a weaker interaction between Al and Cr atoms. These findings contribute to our understanding of the thermodynamics of the Fe-Al-Cr alloy and highlight the favorable conditions for the formation of solid solutions within this alloy system.

The addition of Cr to the Fe-Al composition leads to the most negative value of the formation enthalpy. This implies that converting the Fe-Al alloy to the Fe-Al-Cr alloy requires additional energy and heat, resulting in an increase in the process temperature. The more negative the value of ΔH, the stronger the bond and stability between Fe and Al atoms in the presence of Cr. This indicates that the connection between Fe, Al, and Cr atoms becomes more difficult to break, making the formation of the ternary Fe-Al-Cr alloy more challenging.

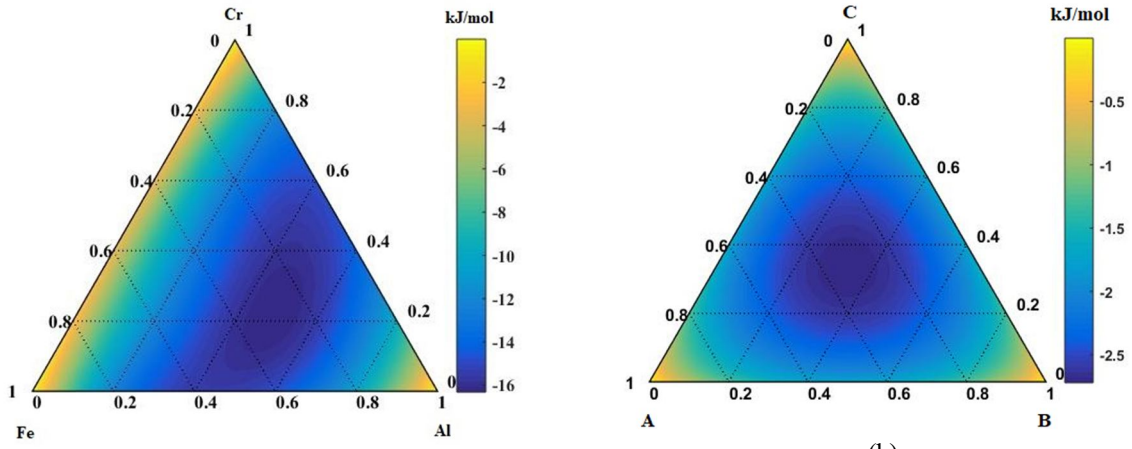

(a) (b)

FIG. 2. (a) Gibbs free energy of Fe-Al-Cr alloys. (b) Ideal Gibbs free energy.

3.2 Fe-Al-Cu Alloy

The information presented in Fig. 3 and Table 3 provides insights into the ΔG for the Fe-Cu and Al-Cu alloys. In the Fe-Cu system, the Gibbs free energy changes with mole fraction, with the highest values occurring near a mole fraction of 50%. This indicates limited solubility of Cu in α-iron under equilibrium conditions, as evidenced by the high positive values of Gibbs free energy. Such high positive values suggest that the formation of Fe-Cu alloys is thermodynamically unfavorable.

Conversely, in the Al-Cu alloy, the most negative value of the ΔG is observed. This indicates a thermodynamic driving force for the formation of the Al-Cu phase, with the system tending to release stored energy to achieve this phase. The negative Gibbs free energy implies that the formation of Al-Cu alloys is thermodynamically favorable.

However, it is worth noting that despite the small atomic radii mismatch between Cu and Fe, the positive ΔG value of Cu with Fe (11.23 kJ/mol) makes the formation of Fe-Cu alloy challenging and impractical within the context of Miedema's model used in the MAAT program. This suggests that there are additional factors beyond atomic radii considerations that impede the formation of Fe-Cu alloy according to this specific model.

It is important to emphasize that these conclusions are drawn from theoretical predictions based on thermodynamic calculations using Miedema's model. Experimental validation is necessary to confirm these findings and to assess the real-world feasibility of forming Fe-Cu alloys. Furthermore, factors such as kinetic barriers, processing parameters, and alloying effects must also be considered when evaluating the practical viability of alloy formation.

TABLE 3. Gibbs free energy in kJ/mol and atomic size mismatch for Fe-Cu and Al-Cu.

Binary alloy	(ΔG) [kJ/mol]	Atomic size mismatch %
Fe-Cu	11.23	**1.5**
Al-Cu	-6.92	10.4

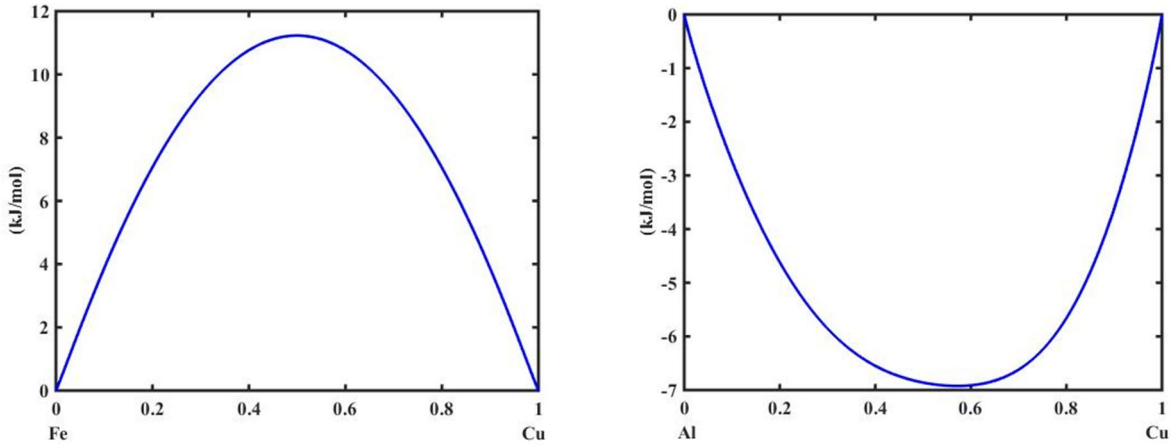

FIG. 3. Gibbs free energy of Fe-Cu and Al-Cu alloys.

The results presented in Fig. 4 indicate that the Fe-Al-Cu alloy exhibits the most negative Gibbs free energy at around a 50% mole fraction of Fe. This suggests that there is a thermodynamic driving force for the formation of the Fe-Al-Cu solid solution from elemental Fe, Al, and Cu. The fact that ΔG is smaller than ΔG^{ideal} further supports the feasibility of forming the ternary alloy through solid solution.

It is worth noting that the largest values of ΔG are observed near the Fe-Al system, indicating that the addition of Cu has a minimal effect on the thermodynamic stability of the Fe-Al-Cu alloy compared to the Fe-Al alloy. However, it is interesting to observe that the incorporation of Cu leads to a less negative value of ΔH for the Fe-Al-Cu alloy compared to the Fe-Al alloy. This suggests that the addition of Cu may influence other factors, such as improving the morphology of the phase boundary and slowing down grain growth, thereby enhancing the thermal stability of the Fe-Al alloy.

These findings have significant implications for the targeted application and desired performance properties of Fe-Al-Cu alloys. Understanding the role of Cu in modifying mechanical, thermal, and corrosion resistance properties is crucial for the alloy's effective use in engineering applications. Additionally, exploring the effects of microstructural features and phase distribution will further clarify the alloy's performance characteristics. It would also be beneficial to compare the thermodynamic results with experimental data, if available, to validate the accuracy and reliability of the theoretical predictions based on Miedema's model and the MAAT software.

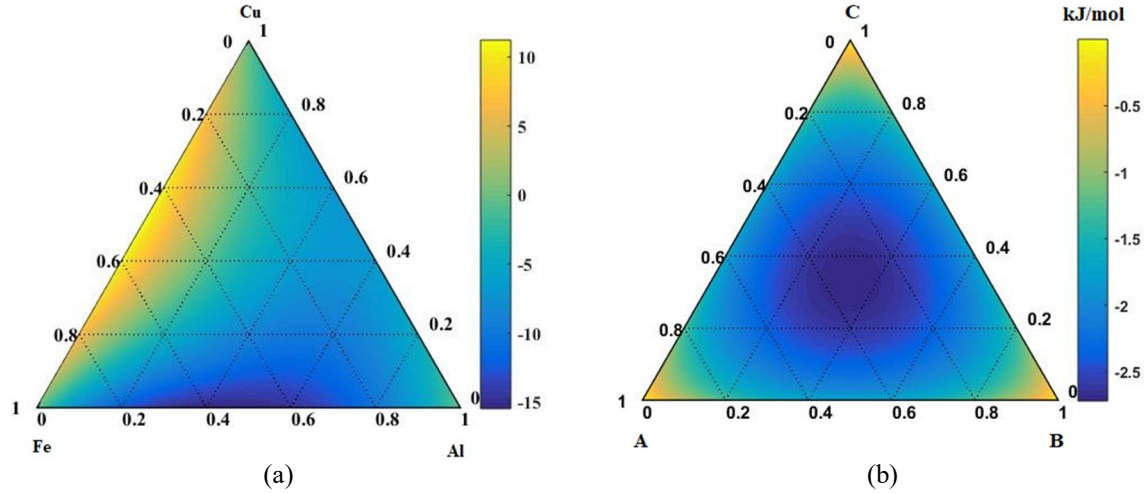

(a) (b)

FIG. 4. (a) Gibbs free energy of Fe-Al-Cu. (b) Ideal Gibbs free energy.

4. Conclusions

The calculations performed using Miedema's model and the MAAT program for the Fe-Al-Cr and Fe-Al-Cu alloys yield interesting results. The inclusion of Cr in the Fe-Al alloy leads to an improvement in the formation enthalpy, indicating a driving force for the formation of the Fe-Al-Cr solid solution. This suggests that the addition of Cr enhances the stability and thermodynamic favorability of the ternary alloy. Similarly, the addition of Cu in the Fe-Al alloy enhances the thermal stability of the alloy. This improvement in thermal stability can be attributed to the influence of Cu on the microstructure and phase distribution of the alloy. The presence of Cu may result in improved phase boundary morphology and hindered grain growth, contributing to increased thermal stability.

It is important to recognize that while these findings from theoretical models like Miedema's model provide valuable insights into the thermodynamic behavior of ternary alloys, experimental validation is necessary to confirm their accuracy and reliability. Further experimental studies could be undertaken to characterize the mechanical, thermal, and other relevant properties of the Fe-Al-Cr and Fe-Al-Cu alloys, thereby supporting and validating the findings obtained from theoretical calculations. Overall, the results suggest that the addition of specific alloying elements such as Cr and Cu can significantly influence the thermodynamic properties and thermal stability of Fe-Al-based ternary alloys. This knowledge can be applied in the design and optimization of these alloys for various engineering applications where stability, strength, and high-temperature performance are crucial factors to consider.

References

[1] Ouyang, Y., Zhong, X., Du, Y., Jin, Z., He, Y., and Yuan, Z., J. Alloys Compd., , 416 (1-2) (2006) 148.

[2] Zhang, R.F., Sheng, S.H., and Liu, B.X., Chem. Phys. Lett., 442 (4-6) (2007) 511.

[3] Niessen, A.K. et al., Calphad, 7 (1) (1983) 1.

[4] Al-Mathami, A., "Crystal Structure and Oxidation Behavior of Al-Containing Stainless-Steel Coatings Produced by Cryomilling and Spark Plasma Sintering", (2010).

[5] Jönsson, B., Berglund, R., Magnusson, J., Henning, P., and Hättestrand, M., Mater. Sci. Forum, 461 (2004) 455.

[6] Aghili, S.E., Enayati, M.H., and Karimzadeh, F., Mater. Manuf. Process., 27 (4) (2012) 467.

[7] Liu, H., Tang, W., Wang, Y., Liu, C., Xu, G., and Zheng, Z., J. Alloys Compd., 506 (2) (2010) 963.

[8] Göğebakan, M., Avar, B., and Zun, O., Mater. Sci., 27 (3) (2009) 0137.

[9] Bloom, P.D., Baikerikar, K.G., Otaigbe, J.U., and Sheares, V.V., Mater. Sci. Eng. A, 294 (2000) 156.

[10] Schwartz, C.J., Bahadur, S., and Mallapragada, S.K., Wear, 263 (7-12) (2007) 1072.

[11] Tcherdyntsev, V.V., Sviridova, T.A., Shevchukov, A.P., and Kaloshkin, S.D., Z. Kristallogr., 223 (11-12) (2008) 751.

[12] Mitka, M., Lityńska-Dobrzyńska, L., Góral, A., and Maziarz, W., Acta Phys. Pol. A, 126 (4) (2014).

[13] Travessa, D.N., Cardoso, K.R., Wolf, W., Jorge Junior, A.M., and Botta, W.J., Mater. Res., 15 (2012) 749.

[14] Tcherdyntsev, V.V., Kaloshkin, S.D., Salimon, A.I., Tomilin, I.A., and Korsunsky, A.M., J. Non-Cryst. Solids, 312 (2002) 522.

[15] Miedema, A.R., De Chatel, P.F., and De Boer, F.R., Physica B + C, 100 (1) (1980) 1.

[16] Aaronson, H.I., Enomoto, M., and Lee, J.K., "Mechanisms of Diffusional Phase Transformations in Metals and Alloys", (CRC Press, 2016).

[17] Callister Jr, W.D. and Rethwisch, D.G., "Fundamentals of Materials Science and Engineering: An Integrated Approach", (John Wiley & Sons, 2020).

[18] Wang, R.N., He, Y., and Feng, J.Y., Nucl. Instrum. Methods Phys. Res. B, 222 (3-4) (2004) 462.

[19] Chelikowsky, J.R., Phys. Rev. B, 25 (10) (1982) 6506.

[20] Zhang, R.F., Zhang, S.H., He, Z.J., Jing, J., and Sheng, S.H., Comput. Phys. Commun., 209 (2016) 58.

[21] Li, H., Sun, X., and Zhang, S., Mater. Trans., 55 (12) (2014) 1816.

[22] Alsaedi, A.K., Abbas, F.S., Alaboodi, A.S., and Abojassim, A.A., Malays. J. Sci., 41 (3) (2022) 22.

[23] Imani, M. and Enayati, M.H., J. Alloys Compd., 705 (2017) 462.

[24] Basu, J., Murty, B.S., Ranganathan, S., J. Alloys Compd., 465 (1-2) (2008) 163.

[25] Hillert, M., Calphad, 4 (1980) 1.

[26] Aguilar, C., Martinez, C., Tello, K., Palma, S., Delonca, A., San Martín, F., and Alfonso, I., Metals, 10 (4) (2020) 510.

[27] Eshelby, J.D., Appl. Phys., 25 (2) (1954) 255.

[28] Bakker, H., Modder, I.W., and Kuin, M.J., Intermetallics, 5 (7) (1997) 535.